Supplementary Material for

Selective neuronal lapses precede human cognitive lapses following sleep deprivation

Supplementary Table 1. Data acquisition details

Session	Patient	Brain regions monitored	Time	Paradigm	Time spent awake (hours)	Subjective sleepiness (1-10)	Total Clusters	SU	MU	MTL	MTL responsive	Percent
1	P415	RA, REC, RAH, RPHG, ROF, RAC, LA, LEC, LAH, LPHG, LOF, LAC	2pm, before sleep deprivation	1 block (12min)	6	N/A	32	11	21	21	1	5%
2	P415	RA, REC, RAH, RPHG, ROF, RAC, LA, LEC, LAH, LPHG, LOF, LAC	12:30pm, after sleep deprivation	1 block (12min)	26.5	7.0	30	9	21	17	1	6%
3	P415	RA, REC, RAH, RPHG, ROF, RAC, LA, LEC, LAH, LPHG, LOF, LAC	11:30pm	1 block (12min)	15.5	N/A	43	4	39	29	1	3%
4	P422	RAH, RPHG, ROF, RPP, LPHG, LPT, LOF, LAC, LPSMA	21:15pm	1 block (12min)	12.8	5.0	56	18	38	27	4	15%
5	P422	RAH, RPHG, ROF, RPP, LPHG, LPT, LOF, LAC, LPSMA	19:00pm	2 blocks (24min)	9	1.0	41	26	15	12	9	75%
6	P422	RAH, RPHG, ROF, RPP, LPHG, LPT, LOF, LAC, LPSMA	20:30pm	2 blocks (24min)	10	1.0	29	17	12	10	6	60%
7	P423	RA, REC, RMH, ROF, LA, LEC, LMH, LOF	21:00pm	2 blocks (24min)	16	5.0	33	19	14	25	8	32%
8	P424	RFuG, RSTG, RFP, LEC, LMH, LCLFTa, LMC	21:45pm	2 blocks (24min)	14.8	6.5	99	48	51	34	9	26%
9	P424	RFuG, RSTG, RFP, LEC, LMH, LCLFTa, LMC	21:00pm	2 blocks (24min)	12.5	4.0	93	40	53	30	9	30%
10	P424	RFuG, RSTG, RFP, LEC, LMH, LCLFTa, LMC	01:00am, before sleep deprivation	2 blocks (24min)	17.5	5.0	87	47	40	30	4	13%
11	P424	RFuG, RSTG, RFP, LEC, LMH, LCLFTa, LMC	05:30am, after sleep deprivation	2 blocks (24min)	22	7.0	69	27	42	22	4	18%
12	P425	RA, REC, RAH, RPHG, ROF, RAC, LA, LAH, LPHG, LOF	10:30pm, before sleep deprivation	1 block (12min)	10.5	5.0	50	20	30	14	3	21%
13	P425	RA, REC, RAH, RPHG, ROF, RAC, LA, LAH, LPHG, LOF	10:30am, after sleep deprivation	1 block (12min)	21.5	5.0	49	15	34	14	1	7%
14	P426	RA, REC, RSTG, LA, LEC, LSTG, LTPO, ROF, RAC, LAC	20:30pm	2 blocks (24min)	12.5	6.5	118	29	89	25	11	44%
15	P426	RA, REC, RSTG, LA, LEC, LSTG, LTPO, ROF, RAC, LAC	21:30pm	2 blocks (24min)	9.5	7.0	53	5	48	17	1	6%
16	P428	RA, REC, RMH, ROF, RFF, LA, LEC, LMH, LOF, LAC, LPF	17:40pm	1 block (12min)	10.7	N/A	44	13	31	34	0	0%
17	P429	RA, RAH, REC, RPHG, ROF, LA, LAH, LEC, LPHG, LOF	10pm, before regular sleep	2 blocks (24min)	14	8.0	56	4	52	15	10	67%
18	P429	RA, RAH, REC, RPHG, ROF, LA, LAH, LEC, LPHG, LOF	11am, after regular sleep	2 blocks (24min)	3.5	5.0	90	20	70	25	11	44%
19	P432	RAC, RPSMA, LA, LAH, RSMA, ROF	11:25pm, before sleep deprivation	1 block (12min)	17.4	N/A	23	15	8	3	0	0%
20	P432	RAC, RPSMA, LA, LAH, RSMA, ROF	21:30pm, after sleep deprivation	1 block (12min)	26.5	N/A	20	7	13	5	0	0%
21	P432	RAC, RPSMA, LA, LAH, RSMA, ROF	19:44pm	2 blocks (24min)	13.8	4.0	24	10	14	7	0	0%
22	P432	RAC, RPSMA, LA, LAH, RSMA, ROF	19:40pm	2 blocks (24min)	11.7	3.0	16	8	8	4	0	0%
23	P434	ROF, RMH, RA, REC, LOF, LAH, LA, LEC, RAC, RAF, LAC, LAF	19:15pm	2 blocks (24min)	11.3	2.5	58	26	32	30	4	13%
24	P434	ROF, RMH, RA, REC, LOF, LAH, LA, LEC, RAC, RAF, LAC, LAF	21:40pm	1 block (12min)	13.7	3.5	58	27	31	33	0	0%
25	P434	ROF, RMH, RA, REC, LOF, LAH, LA, LEC, RAC, RAF, LAC, LAF	22:55pm	2 blocks (24min)	14.9	4.0	52	25	27	23	0	0%
26	P434	ROF, RMH, RA, REC, LOF, LAH, LA, LEC, RAC, RAF, LAC, LAF	19:40pm	1 block (12min)	11.2	4.0	49	21	28	27	4	15%
27	P434	ROF, RMH, RA, REC, LOF, LAH, LA, LEC, RAC, RAF, LAC, LAF	17:20pm	2 blocks (24min)	9.3	2.5	13	5	8	7	0	0%
28	P475	RAH, REC, RPHG, RPT, RSTG, RTP, LAH, LEC, LMTG, LPT, LSTG, LTP	18:45pm	2 blocks (24min)	9.75	4.5	15	11	4	5	1	20%
29	P475	RAH, REC, RPHG, RPT, RSTG, RTP, LAH, LEC, LMTG, LPT, LSTG, LTP	14:50pm	2 blocks (24min)	9	3.5	27	15	12	12	2	17%
30	P476	REC, RMH, LA, LEC, LMH, LOF, LPHG	19:08pm, before regular sleep	2 blocks (24min)	9	5.5	14	2	12	14	2	14%
31	P476	REC, RMH, LA, LEC, LMH, LOF, LPHG	10:55am, after regular sleep	2 blocks (24min)	4	4.0	40	17	23	40	0	0%
						Total	1481	561	920	611	106	17%

Data acquisition details. Each row shows one experimental session. Columns (left to right) show session number, patient number, list of brain regions monitored (abbreviations below), time of day, which paradigm (either 1 or 2*12-minute blocks, depending on patient), time spent awake before experiment, total number of clusters identified in spike-sorting, number of single-unit clusters, number of multi-unit clusters, number of Medial Temporal Lobe (MTL) units, number of MTL units responsive to at least one picture, and percent of MTL units found to be responsive. Altogether, we recorded from 1481 units (561 single-units, 920 multi-unit clusters). 106 MTL neurons (out of 611, 17%) were responsive to at least one picture used in the experiment. Gray highlights mark the four sessions conducted after complete full-night sleep deprivation.

Abbreviations: RA, Right Amygdala; REC, Right Entorhinal Cortex; RMH, Right Middle Hippocampus; RAH, Right Anterior Hippocampus; RPHG, Right Parahippocampal Gyrus; ROF, Right Orbitofrontal Cortex; RAC, Right Anterior Cingulate Cortex; RPP, Right Posterior Parietal Cortex; RPSMA, Right Pre-Supplementary Motor Area; RSMA, Right Supplementary Motor Area; RFuG, Right Fusiform Gyrus; RSTG, Right Superior Temporal Gyrus; RFP, Right Frontal Posterior; RPT, Right Posterior Temporal; RTP, Right Temporal Parietal; LA, Left Amygdala; LEC, Left Entorhinal Cortex; LMH, Left Middle Hippocampus; LAH, Left Anterior Hippocampus; LPHG, Left Parahippocampal Gyrus; LOF, Left Orbitofrontal Cortex; LAC, Left Anterior Cingulate Cortex; LAF, Left Anterior Frontal; LPT, Left Posterior Temporal; LPSMA, Left Pre-Supplementary Motor Area; LF, Left Frontal; LMC, Left Middle Cingulate; LSTG, Left Superior Temporal Gyrus; LMTG, Left Middle Temporal Gyrus; LPT, Left Posterior Temporal; LTP, Left Temporal Parietal; LTPO, Left Temporo-Parietal-Occipital; LPF, Left Posterior Frontal;

Supplementary Figure 1. Fitting ExGaussian distributions to behavioral RT data and defining cognitive lapses across experimental sessions

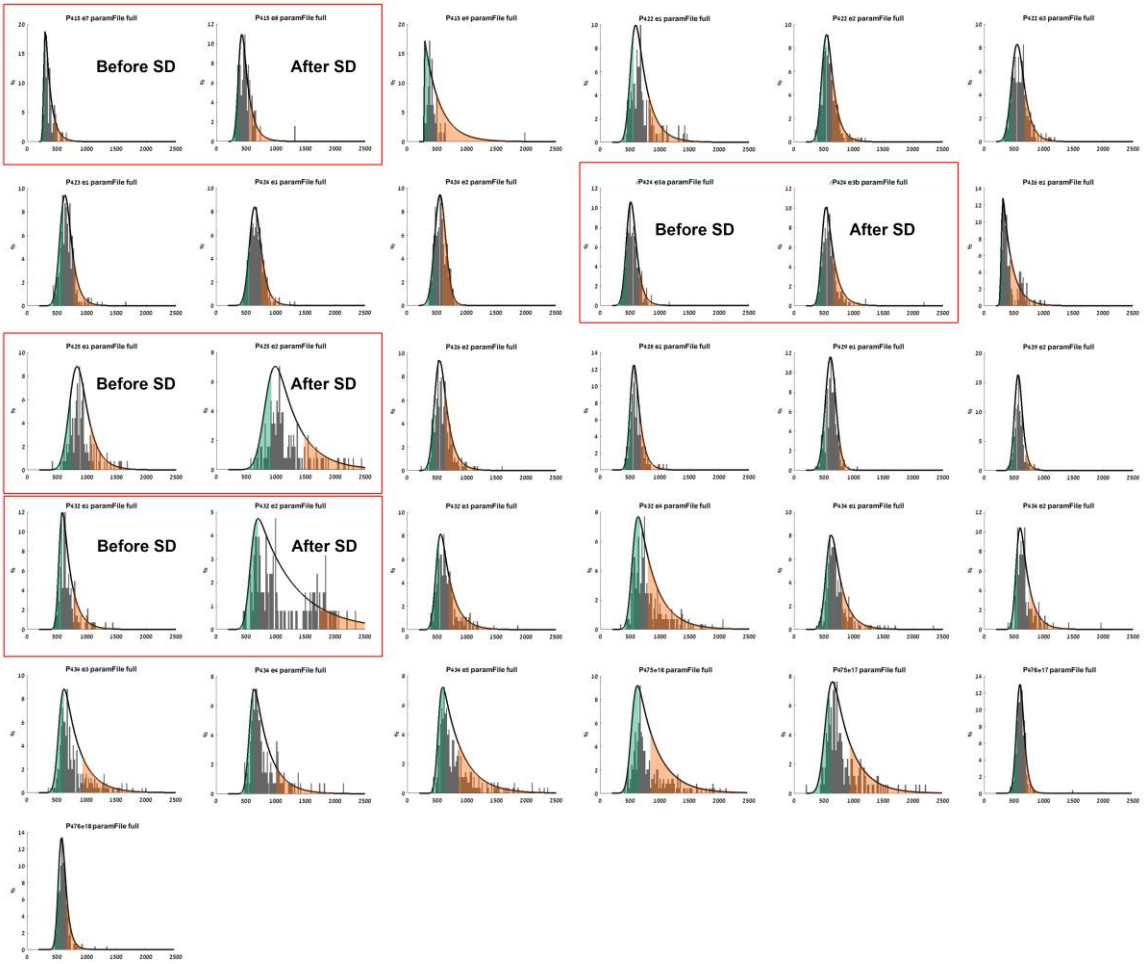

Each subpanel (n=31) shows the distribution of reaction times (RTs) in one experimental session, and the fitting of an ExGaussian distribution. Based on this fit, cognitive lapses (slow trials, orange highlight) were defined as the right tail (values outside the Gaussian distribution; >99.9% of the Gaussian component and within the 20% slowest trials). For comparison of neuronal data, an equal number of trials with the fastest reaction times were defined as 'fast trials' (green highlight). Red rectangles mark the four session pairs conducted before/after full-night sleep deprivation (SD).

Supplementary Figure 2. "Time-on-task" effect

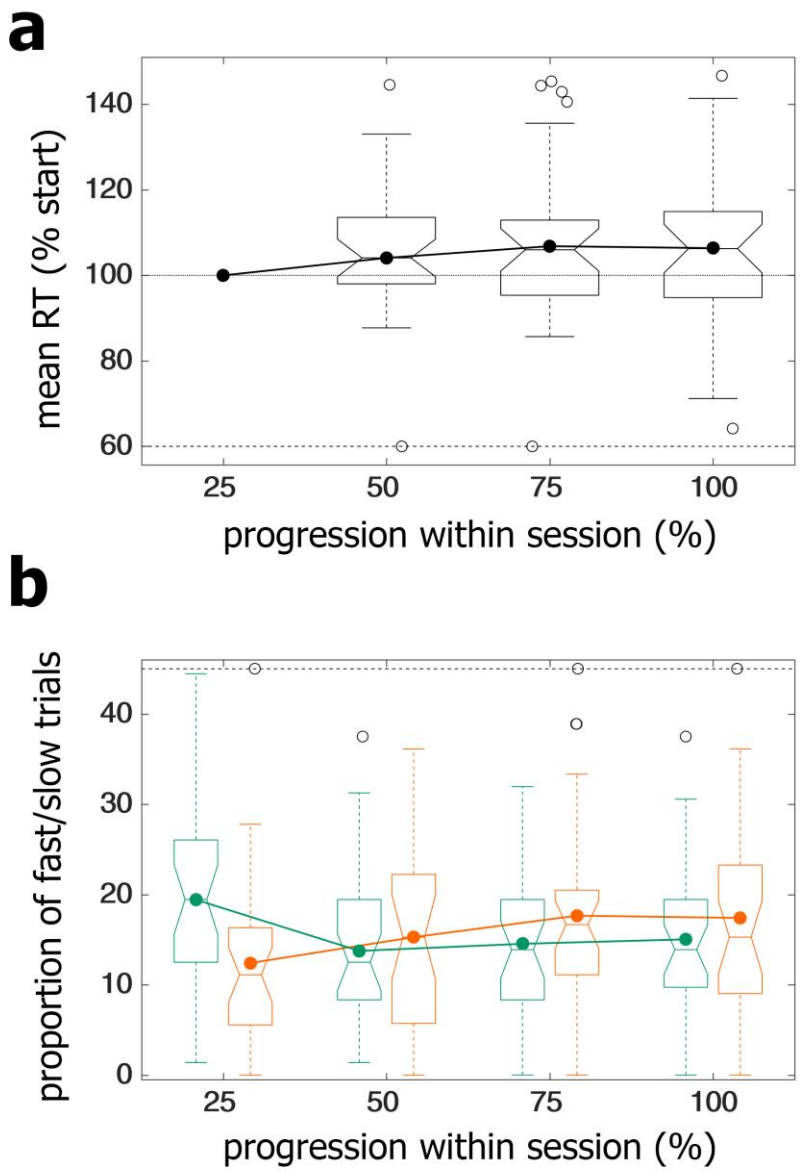

(a) Mean reaction time (RT) during face/non-face categorization PVT sessions, divided by percentile of time progression within the session. Note the trend for increase in mean RT as the session progresses in time, reflecting the "time on task" effect. **(b)** Proportion of 'fast trials' (green) and 'slow trials' (orange), separately by percentile of time progression within the session. Note that as the session progresses in time, the proportion of 'fast trials' decreases while the proportion of 'slow trials' increases. In both panels, full circles and solid lines mark mean values, boxes mark the 25th and 75th percentiles and the median, and whiskers denote min and max values of distribution across recording sessions (n=31) excluding statistically-defined outliers (open circles).

Supplementary Figure 3. Single-trial detection of response onset and termination

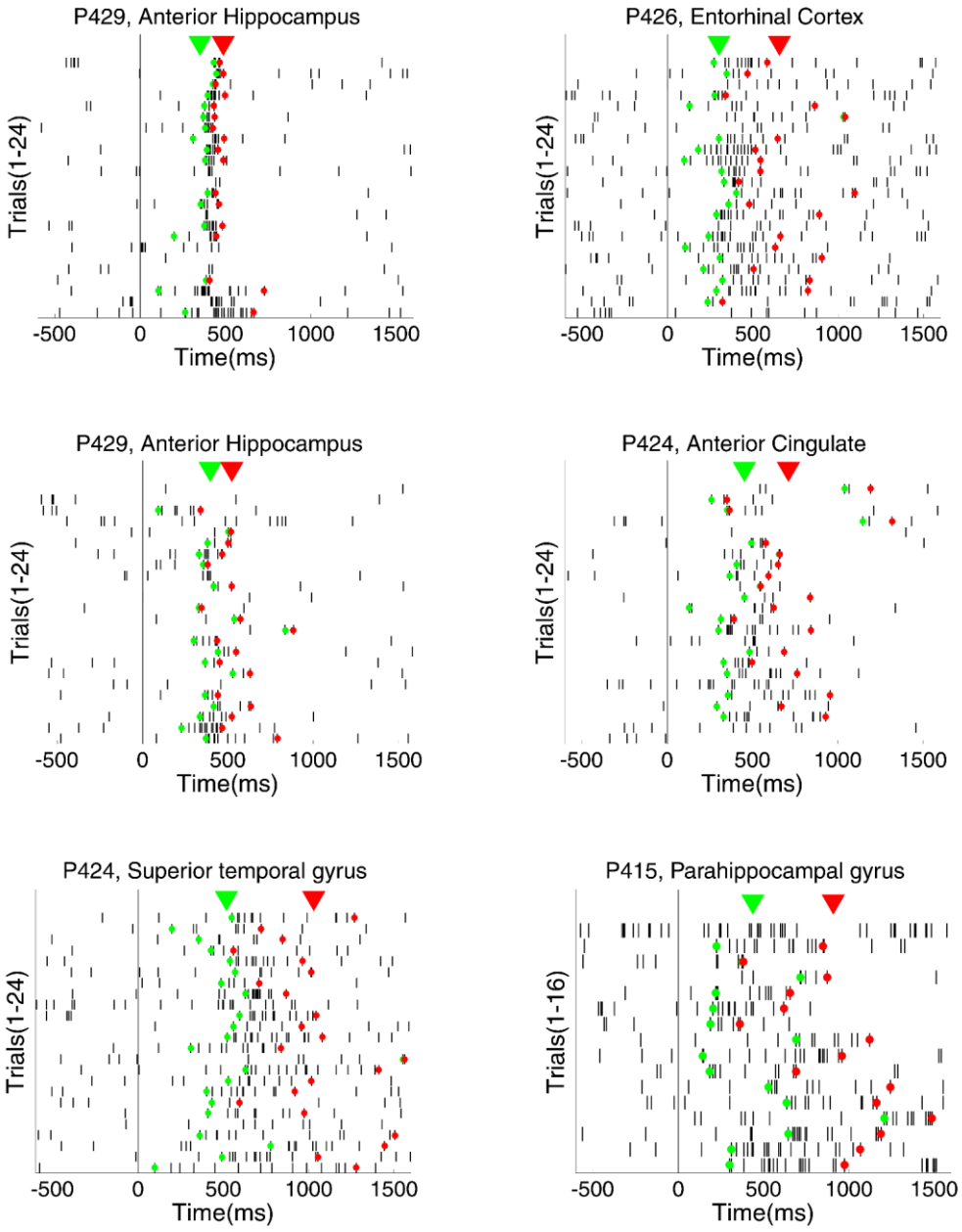

Examples of single-trial response detection. Responses were detected on the basis of significant ($p<0.005$) deviation from Poisson process (λ=baseline firing rate) as described in Online Methods. In trials where a significant response was detected, green/red circles represent response onset/termination. Green/red triangles represent the mean response onset/ termination across trials.

Supplementary Figure 4. Latency and selectivity of neuronal responses per region

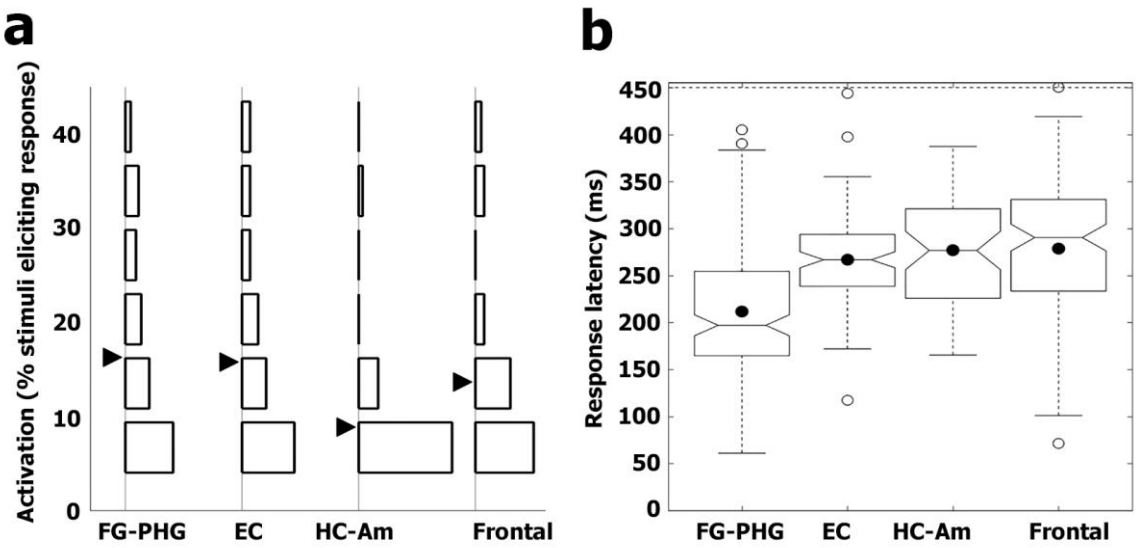

(a) Single-unit responsiveness per region: a given unit was declared responsive for a given picture whenever its firing rate 200-500ms after stimulus onset was significantly greater than baseline (-600-0ms, $p < 0.005$ via paired t-test). For all units responsive to at least one picture (n=168), we computed the number of pictures to which it responded and divided it by the number of presented images ("Activation", y-axis). The mean (black triangles) and distribution (bars along the y-axis) depict the activation values for each region (x-axis). Note that neurons in hippocampus/amygdala are associated with highest selectivity (activated by few images) compared with neurons in other regions. Abbreviations: FG, Fusiform Gyrus; PHG, Parahippocampal Gyrus; EC, Entorhinal Cortex; HC, hippocampus; Am, Amygdala; Frontal, frontal lobe **(b)** Response latency per region: for each unit, we focused on trials in which images eliciting significant activations were presented. For each of these trials, an automatic detection was performed (Methods, Supp. Fig. 3 and Fig. 3a) and when a response was detected, its latency (from stimulus onset) was extracted. Full black circles mark mean latency values in each brain region (x-axis), boxes mark the median and the 25th and 75th percentiles, and whiskers denote min and max values of distribution across unit responses excluding statistically-defined outliers (open circles). Note that average latencies progressively increase along the visual-mnemonic hierarchy (FG/PHG -> EC -> HC/Am). FG-PHG: 159 pictures in 44 units; EC: 104 pictures in 29 units; HC-Am: 53 pictures in 30 units; Frontal: 116 pictures in 40 units. Abbreviations as in panel (a).

Supplementary Figure 5. Spiking activity of non-responsive MTL neurons

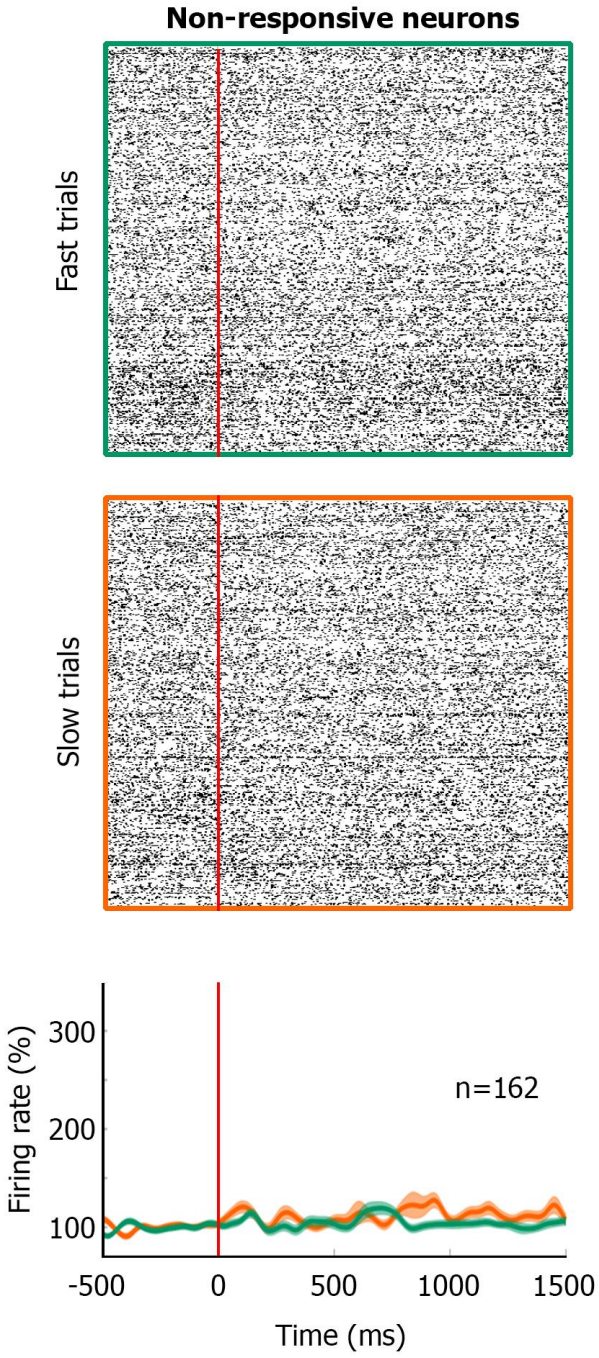

Spiking activity (raster and PSTH) across non-responsive neurons (n=162 randomly selected from the non-responsive neurons recorded simultaneously in the same brain region) during fast trials (top, green) and slow trials (orange, bottom). Note that (a) non-responsive neurons do not show significant modulations after image presentation attesting to their correct classification, and (b) effects of lapses are not evident in the spiking activity of these neurons.

Supplementary Figure 6. Comparing neuronal spiking activity in fast trials vs. slow trials in each patient separately

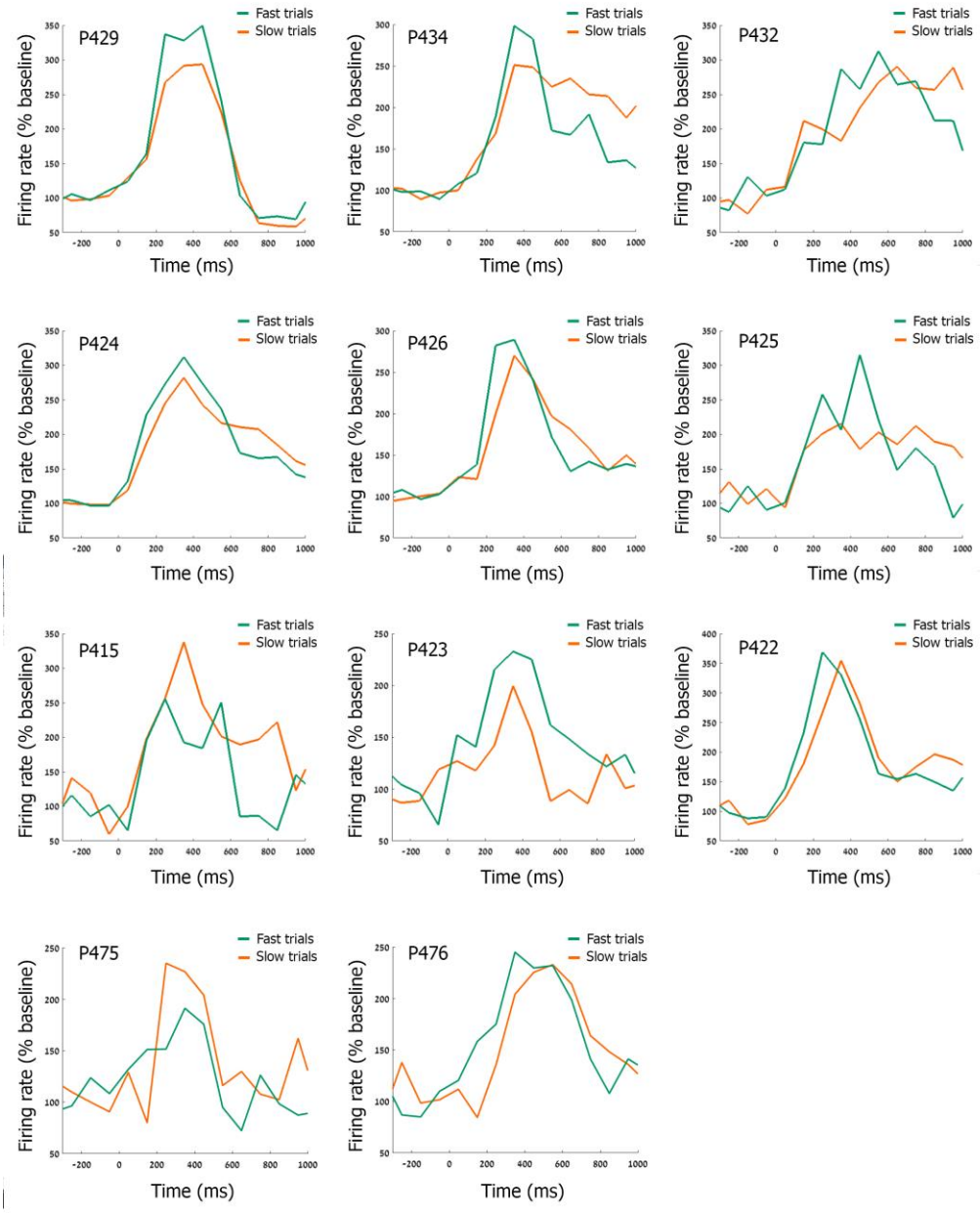

Average spiking responses (peri-stimulus-time-histogram, PSTH) for each one of the eleven participants in whom spiking activities were recorded. Green, fast trials; Orange, slow trials. PSTH are binned in 100ms bins. Note that in 9 out of 11 individuals, spiking activity in the same neurons in response to identical stimuli during slow trials was associated with attenuated and/or delayed response.

Supplementary Figure 7. Comparison of stimulus-locked and response-locked averaging of neuronal spiking responses

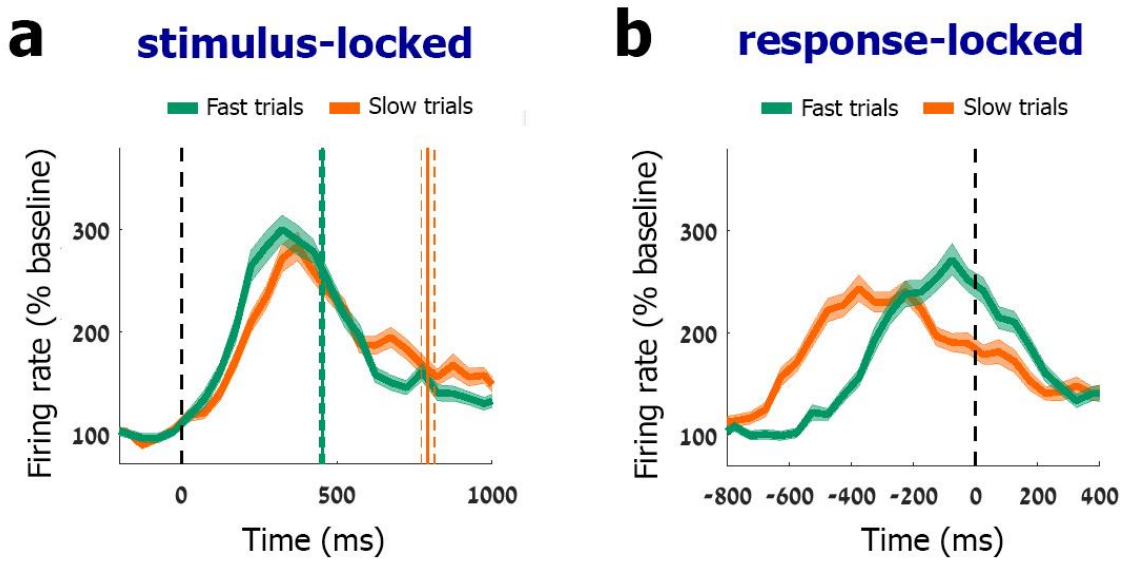

(a) Peri-stimulus-time-histogram (PSTH) of neuronal spiking responses in responsive units (n=469 pictures in 162 units). Black vertical dashed line marks stimulus onset (time zero); green vertical solid and dashed lines mark average ± SEM timing of behavioral response (button press) in fast trials with lowest RTs; orange vertical solid and dashed lines mark average ± SEM timing of behavioral response in slow trials (cognitive lapses) with low RTs. PSTH is smoothed with a Gaussian kernel with σ = 30ms. **(b)** Same neuronal data averaged around behavioral button press ("response-locked"). Note that neuronal activity is more tightly linked with stimulus onset than with behavioral response.

Supplementary Figure 8. Correlation between response latency and reaction times (RT) across ALL trials

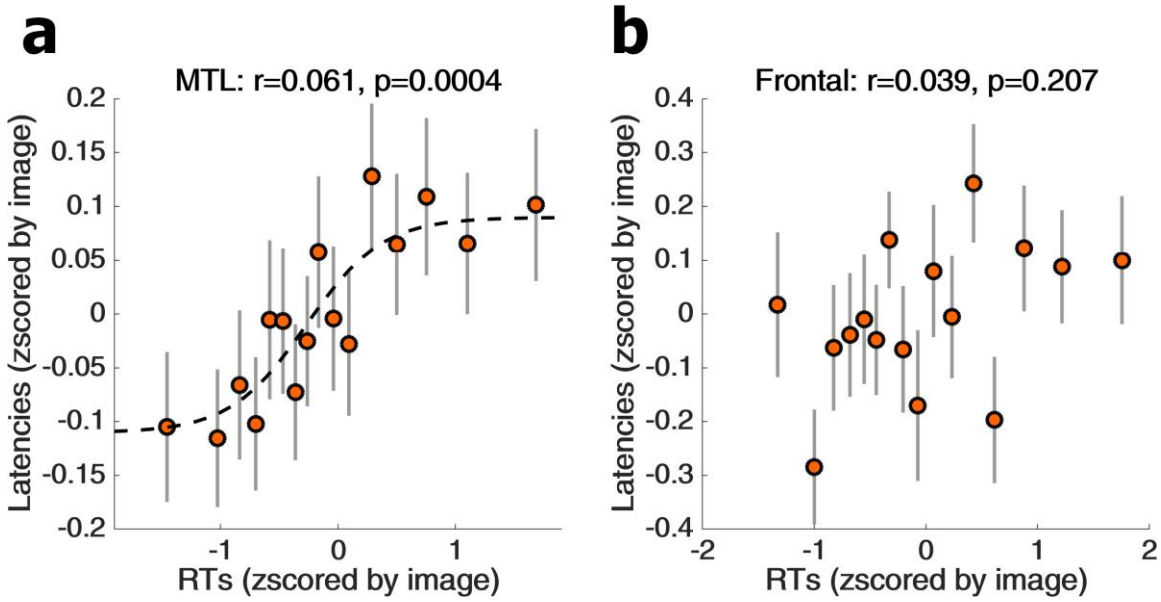

(a) Scatter plot of normalized response latency (y-axis) vs. normalized reaction times (RTs, x-axis) in the Medial Temporal Lobe (MTL). For each neuron and picture that elicited a significant response, response latency was extracted and normalized (z-score across trials and units) and compared with normalized reaction times in that session. Trials (n=3327) were then aggregated in 17 bins sorted by increasing RTs to facilitate visualization. A significant correlation (r=0.061, $p=4.2*10^{-4}$) was observed when calculated on all trials before binning. Note that the relation between response latency and RTs is best fit by a sigmoidal (rather than linear) model, supporting the notion that lapses may represent a qualitatively distinct subset of trials. **(b)** Same for normalized response latency (y-axis) vs. normalized reaction times (RTs, x-axis) in the frontal lobe. No significant correlation (r=0.039, p =0.207, n=1075) was observed when calculated on all trials before binning. Error bars in both panels denote the standard error of the mean (SEM) computed across trials for each bin.

Supplementary Figure 9. Single-trial examples of weakened decrease in slow/theta LFP power during slow trials (cognitive lapses)

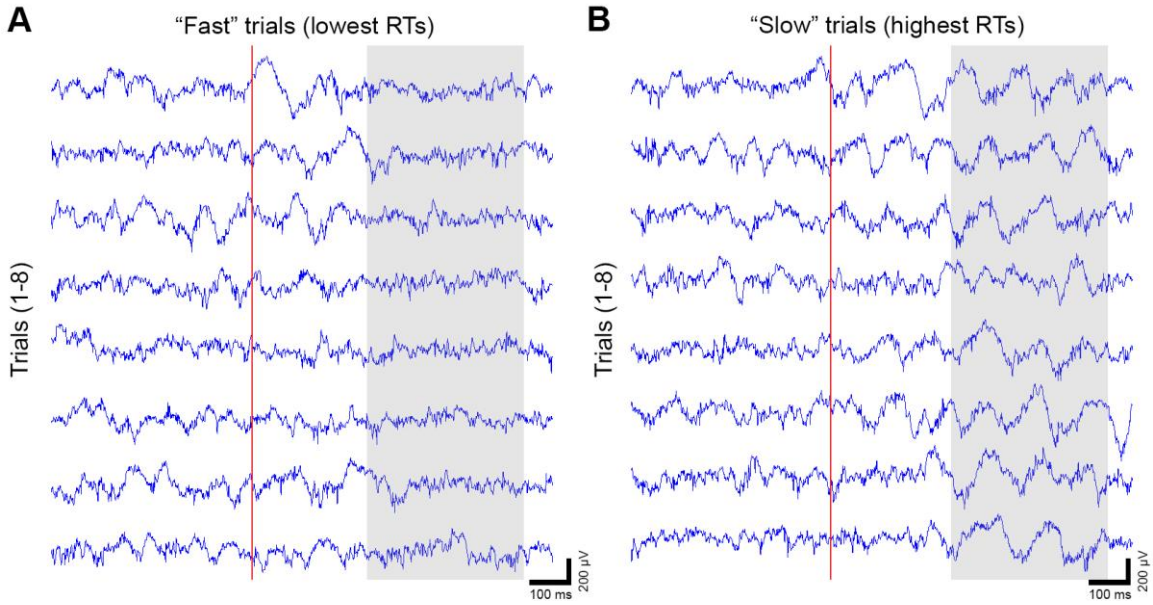

(A) Raw unfiltered LFP traces recorded in the right entorhinal cortex around "fast" trials (lowest RT) and **(B)** "slow" trials (highest RT) in the same recording session. Rows denote 8 representative trials for each category. Vertical red line, trial onset. Note that during fast trials, the interval 300-700ms after trial onset (gray shading) is associated with an increase in high frequency power and a decrease in slow/theta power, whereas during slow trials (cognitive lapses) there is less decrease in slow/theta power.

Supplementary Figure 10. Comparing power of evoked LFP (averaged across trials) in fast trials vs. slow trials

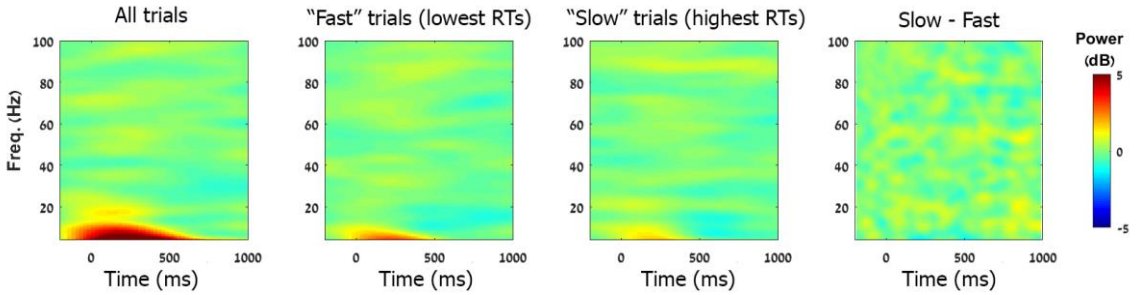

Time-frequency decomposition of evoked power changes (power of the average event-related LFP) in MTL responsive channels (n=268 channels in 31 sessions). Columns (left to right) denote evoked power changes for all trials, fast trials, slow trials (cognitive lapses), and difference between slow and fast trials. In each subpanel, hot and cold colors mark increases and decreases in power compared to baseline, respectively. Note that evoked power consists of an increase in slow/theta (2-10Hz) power in the first 500ms after stimulus onset that is significantly greater during fast trials ($p=0.0012$ via Wilcoxon signed-rank test). This effect (more power during fast trials) is opposite to the 'induced' power effects at those frequencies (pink rectangle in Figure 4, less power during fast trials), suggesting that decreases in induced power changes do not reflect changes in the event-related potential, but may stem from changes in ongoing activity.

Supplementary Figure 11. Baseline theta power and its relation to sleepiness and cognitive lapses

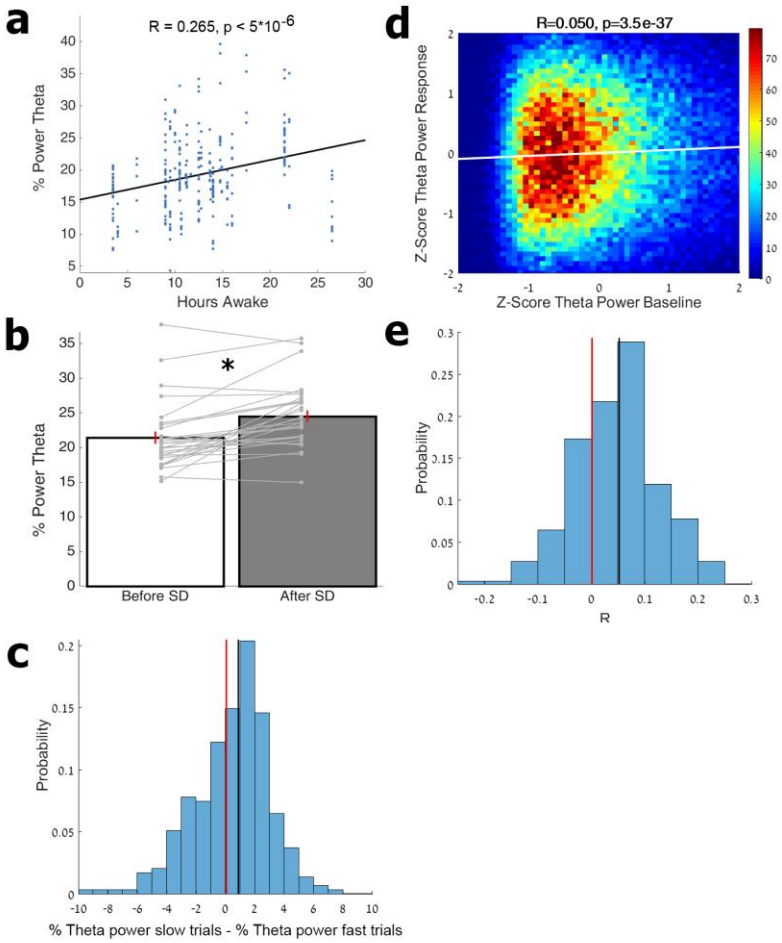

(a) Scatter plot between percent power contained in the theta (6-10Hz) band during baseline periods (ordinate, y-axis) and time spent awake before each session (abscissa, x-axis) reveals significant correlation (r=0.26, $p<5*10^{-6}$, N=295 LFP channels) indicating increased theta activity with increasing sleep pressure. **(b)** Percent power contained in the theta (6-10Hz) band during baseline periods is higher in sessions conducted after full-night SD (right) compared with sessions before SD (left), (*, $p<2.74*10^{-5}$, via Wilcoxon signed-rank test). Red error-bars denote SEM across LFP channels (n=31). Gray dots and lines mark individual channels. **(c)** Distribution of differences between theta (6-10Hz) power prior to slow trials vs. theta power prior to fast trials shows a significant elevation in theta power dominance prior to slow trials ($p<0.0001$ via Wilcoxon signed-rank test, N=295 LFP channels). Vertical red line denotes zero difference while vertical black line denotes median of actual data (at 0.89%). **(d)** Scatter plot between percent power contained in the theta (6-10Hz) band during baseline periods (ordinate, y-axis) and percent power contained in the slow/theta (2-10HZ) band during the response interval (abscissa, x-axis) reveals modest albeit highly significant correlation (r=0.05, $p<4*10^{-37}$) suggesting that, within each LFP channel, increased baseline theta power and increased slow/theta power during the response interval (as seen in main Figure 4) are related. Both values are normalized (z-score) within each channel to go beyond inter-channel variability. **(e)** Distribution of correlation coefficients within each LFP channel between baseline theta power and response slow/theta power ($p<2*10^{-21}$ via Wilcoxon signed-rank test, N=295 LFP channels). Vertical red line denotes zero difference while vertical black line denotes median of actual data (R=0.052).

Supplementary Figure 12. Quantifying the rate of epileptiform inter-ictal spikes (IIS) around fast trials and slow trials (cognitive lapses)

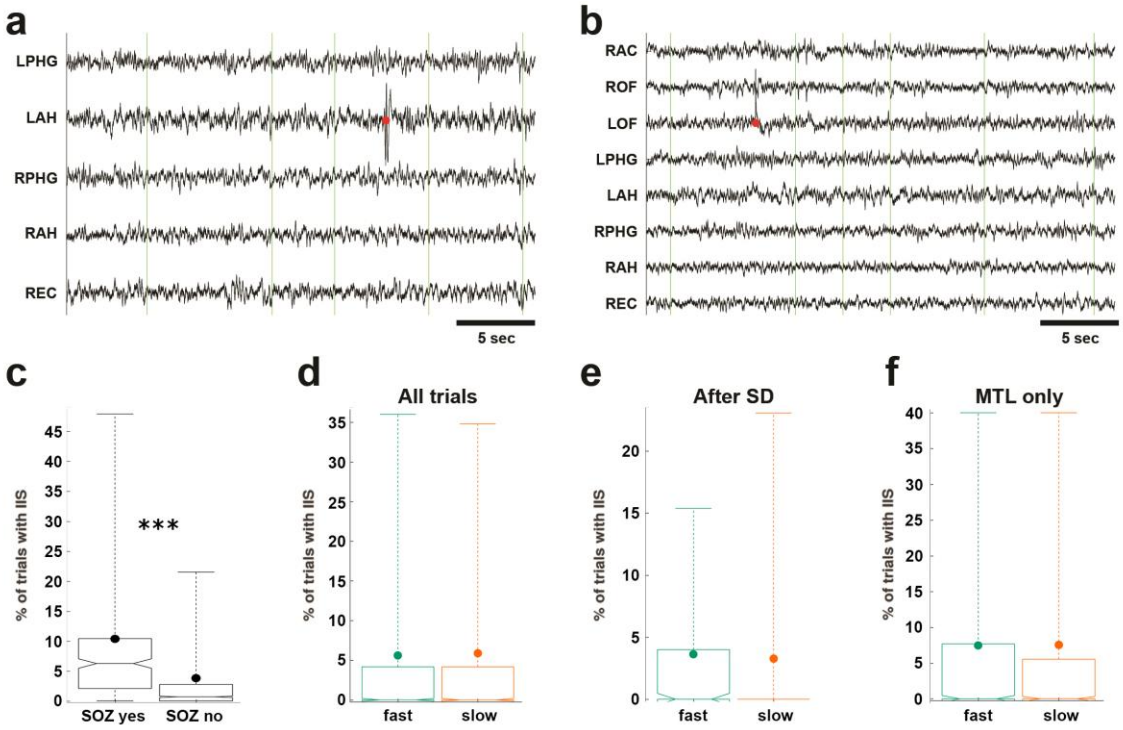

(a) Representative 30sec segment of local field potential data recorded simultaneously in 5 brain regions during the PVT experiment. Red circle, detected IIS event (see Methods for detection details). Vertical green lines, trial onsets. LPHG, left parahippocampal gyrus; LAH, left anterior hippocampus; RPHG, right parahippocampal gyrus; RAH, right anterior hippocampus; REC, right entorhinal cortex. **(b)** Another representative 30sec segment recorded in a different individual. Red circle and vertical green lines as above. RAC, right anterior cingulate; ROF, right orbitofrontal cortex; LOF, left orbitofrontal cortex; **(c)** percent of trials with IIS detected within [-2, 4]sec around trial onset, separately for regions eventually determined to be within or outside the seizure onset zone (SOZ). Note that IIS occurrence in SOZ channels (n=290) was 2.7 times higher (***, $p<10^{-48}$ via Mann-Whitney U-test) than in other regions (n=1358 channels), attesting to successful detection of IIS events. **(d)** Percent of trials with IIS detected within [-2, 4]sec around trial onset, separately for fast trials (green) or slow trials (orange). Note that slow trials (cognitive lapses) were not associated with increased IIS occurrence (p=0.46 via Wilcoxon signed-rank test, N=1533 channels). (e) Percent of trials with IIS detected within [-2, 4]sec around trial onset, separately for fast trials (green) or slow trials (orange) only in sessions conducted after complete sleep deprivation (SD). Slow trials were associated with *decreased* IIS occurrence (p=0.025 via Wilcoxon signed-rank test, N=186 channels). (f) Percent of trials with IIS detected within [-2, 4]sec around trial onset, separately for fast trials (green) or slow trials (orange) only in the medial temporal lobe (MTL) where responsive neuronal circuits exhibited activity changes around cognitive lapses. Slow trials were not associated with increased IIS occurrence (p=0.48 via Wilcoxon signed-rank test, N=619 channels). In panels (c-f) full circles mark mean values, boxes mark the median and the 25th and 75th percentiles, and whiskers denote the 5th and 95th percentiles of distribution across channels.